Superconductor Science and Technology

A renormalised Hamiltonian approach to a resonant valence bond wavefunction

Supercond. Sci. Technol. 1 (1988) 36–46. Printed in the UK

A renormalised Hamiltonian approach to a resonant valence bond wavefunction

F C Zhang, C Gros, T M Rice and H Shiba†
Theoretische Physik, ETH-Hönggerberg, CH 8093 Zurich, Switzerland

Received 1 March 1988, in final form 22 April 1988

Abstract. The effective Hamiltonian of strongly correlated electrons on a square lattice is replaced by a renormalised Hamiltonian and the factors that renormalise the kinetic energy of holes and the Heisenberg spin–spin coupling are calculated using a Gutzwiller approximation scheme. The accuracy of this renormalisation procedure is tested numerically and found to be qualitatively excellent. Within the scheme a resonant valence bond (RVB) wavefunction is found at half-filling to be lower in energy than the antiferromagnetic state. If the wavefunction is expressed in fermion operators, local SU(2) and U(1) invariance leads to a redundancy in the representation. The introduction of holes removes these local invariances and we find that a d-wave RVB state is lowest in energy. This state has a superconducting order parameter whose amplitude is linear in the density of holes.

1. Introduction

Very soon after the discovery of high-T_c superconductivity Anderson [1] proposed that it was caused by a cooperative condensation of carriers moving in a resonant valence bond (RVB) state of spins. Since then this proposal has been studied extensively and the best account is in Anderson's recent lecture notes [2]. Many other proposals have been made (for a Review see [3]), and there have been questions raised about the use of the simplified effective Hamiltonian derived from a single-band Hubbard model in the atomic limit that forms the starting point of Anderson's treatment. We shall not go into these questions here but just point out that two of us (Zhang and Rice [4]) recently gave an explicit demonstration that a two-band model describing hybridised copper 3d and oxygen 2p states can also be reduced to the same effective Hamiltonian in an appropriate limit.

The effective Hamiltonian contains the strict local constraint which forbids double occupancy of any site. This constraint is very difficult to handle analytically. One of the most physically transparent methods to treat this type of problem analytically has been the Gutzwiller approximation which introduces a renormalisation of the quantum mechanical expectation values by a classical weighting factor [5]. Such renormalisation can then be incorporated into a Hamiltonian which may be treated by conventional methods. This approach was used for the heavy fermion problem by Rice and Ueda [6] and was shown to be equivalent to an optimal slave-boson formulation by Kotliar and Ruckenstein [7]. In this paper we will consider this renormilisation Hamiltonian method for the effective Hamiltonian. Unlike the renormalised Anderson Hamiltonian studied by Rice and Ueda [6], in the present case the renormalised Hamiltonian cannot be simply diagonalised and we must resort to a further mean-field approximation. Mean-field approaches have been considered by many authors [8–10]. Here we choose to formulate the problem in terms of a variational wavefunction. This has several advantages. First it shows us that a consistent mean-field theory must be formulated in terms of two expectation values i.e. one must include particle–hole amplitudes of the form $\langle c^+c\rangle$ in addition to particle–particle amplitudes of the form $\langle c^+c^+\rangle$. This point has been recently realised by others as well [11]‡. The coupled equations to minimise the energy have a wide class of degenerate solutions at half-filling. Secondly a wavefunction formulation is suited to examining the role of the redundancy in the fermion representation which is not present in the spin representation. At half-filling, this redundancy which has its origin in the reduction from 4 to 2 degrees of freedom per site as one goes from fermion to spin representation, appears as a local particle–hole (SU(2)) and gauge (U(1)) invariance. The large degeneracy of the mean-field description arises from this redundancy and it can be shown that it corresponds to the *same* state in the spin representation. Further the appearance of coherence in the fermion representation is illusory so that there can be no true phase coherence as stressed by Baskaran and Anderson [12]. Thirdly, this formulation allows a direct comparison with the variational Monte Carlo (VMC) results. This allows us on the one hand to check the

† Permanent Address: Institute for Solid State Physics, University of Tokyo, Roppongi, Tokyo 106, Japan.

‡ In [8], Baskaran and co-workers considered the term $\langle c^+c\rangle$ as well. However they set it equal to zero in their calculations.

0953-2048/88/010036 + 11 $02.50

validity of the renormalised mean-field theory and on the other hand it gives us more insight into the numerical VMC results. Both qualitatively and even quantitatively good agreement is found; for example both point to a d-wave paired state as the most stable and a true superconductivity order parameter which vanishes at half-filling and grows linearly in the deviation from half-filling. The largest discrepancy occurs for the antiferromagnetic state which, within this scheme is higher in energy than the RVB state, contrary to the VMC results.

Our treatment is essentially limited to zero temperature and the extension to finite temperature will be non-trivial. Some discussion of the problems of calculating excitation energies is given. In particular there are two energy scales of excitations given by the gauge coherence energy (determined by the kinetic energy) and the magnetic coherence energy respectively. Anderson [2] has emphasised this splitting of the charged excitations (holons) and spin excitations (spinons).

2. The model and the renormalised Hamiltonian

We study the Hubbard model on a square lattice. In the limit of large on-site Coulomb repulsion U and at one-half, or, slightly less, filling the Hubbard Hamiltonian can be transformed to the form

$$H = H_t + H_s$$
$$H_t = -t \sum_{\langle i,j\rangle,\sigma} c^\dagger_{i\sigma} c_{j\sigma} + \text{HC} \tag{1}$$
$$H_s = J \sum_{\langle i,j\rangle} \boldsymbol{S}_i \cdot \boldsymbol{S}_j$$

with the local constraint the number of electrons on any site $\leqslant 1$. This transformation has a long history, and has been used by [13], amongst others. In (1) H_t and H_s are the kinetic and magnetic energies respectively and $\langle i,j\rangle$ represent the nearest-neighbour pairs. $\boldsymbol{S}_i$ are the spin $= \frac{1}{2}$ operators and $J = 4t^2/U$. We neglect terms which are higher order in the small parameters t/U and the hole concentration $\delta\,(= 1-n$; where n is the electron concentration).

Since the high-T_c superconducting materials show strong antiferromagnetic (AF) spin correlations [14] it is believed that this model contains the essential physics for the high-T_c superconductivity [2, 4].

To study the ground state and the excited states of (1), we use a projected BCS trial wavefunction as suggested by Anderson [1] for a RVB state:

$$|\varphi\rangle = P_d |\varphi_0\rangle \tag{2}$$
$$|\varphi_0\rangle = \prod_k (u_k + v_k c^\dagger_{k\uparrow} c^\dagger_{-k\downarrow})|0\rangle \tag{3}$$

where the Gutzwiller projection operator $P_d = \Pi_i (1 - n_{i\uparrow} n_{i\downarrow})$, and $|0\rangle$ is the vacuum state. u_k and v_k are the variational parameters satisfying the normalisation condition for $|\varphi_0\rangle$: $|u_k|^2 + |v_k|^2 = 1$.

Some special forms of (2) have recently been studied numerically. Using the VMC technique, which treats the projection operator exactly [15–19], the energies of these states have been numerically calculated. It is found that in the square lattice, the projected Fermi liquid state (i.e. the state with $u_k v_k^* = 0$) is unstable against d-wave pairing [16]. At half-filling the energy of the d-wave state is found [17] to be very close to the ground-state energy extrapolated from the exact small system calculations [20]. In contrast to the extrapolated exact small system calculations, the d-wave trial wavefunction has no long range antiferromagnetic order [17] and may therefore be viewed as an example of a quantum spin liquid. A VMC study of superconductivity has been made independently by Yokoyama and Shiba [19]. They also concluded a possibility of a d-wave superconductivity.

The projected BCS wavefunction is a natural generalisation of the usual BCS state to strongly correlated systems. The projection operator, however, makes difficulties for an analytic approach. In this paper we shall use a renormalised Hamiltonian approach to treat the projection operator, and systematically investigate the state (2), carrying out explicitly the variational procedure. In this approach following Gutzwiller [5] the effect of the projection operator on the doubly occupied sites is taken into account by a classical statistical weighting factor which multiplies the quantum coherent result calculated with $|\varphi_0\rangle$. A clear description of the method has been given by Vollhardt [21]. The hopping energy and the spin–spin correlation of the nearest-neighbour sites in the state $|\varphi\rangle$ are related to those in the state $|\varphi_0\rangle$ by

$$\langle c^\dagger_{i\sigma} c_{j\sigma}\rangle = g_t \langle c^\dagger_{i\sigma} c_{j\sigma}\rangle_0$$
$$\langle \boldsymbol{S}_i \cdot \boldsymbol{S}_j\rangle = g_s \langle \boldsymbol{S}_i \cdot \boldsymbol{S}_j\rangle_0$$

where $\langle A\rangle_0$ and $\langle A\rangle$ are the expectation values in the states $|\varphi\rangle_0$ and $|\varphi\rangle$ respectively. The renormalisation factors g_t and g_s are determined by the ratios of the probabilities of the corresponding physical processes in the states $|\varphi\rangle$ and $|\varphi_0\rangle$. In figure 1 we illustrate the possible hopping processes in these two states. The probability of such a process in the state $|\varphi\rangle$ is

$$[n_{j\uparrow}(1 - n_i) n_{i\uparrow}(1 - n_j)]^{1/2}$$

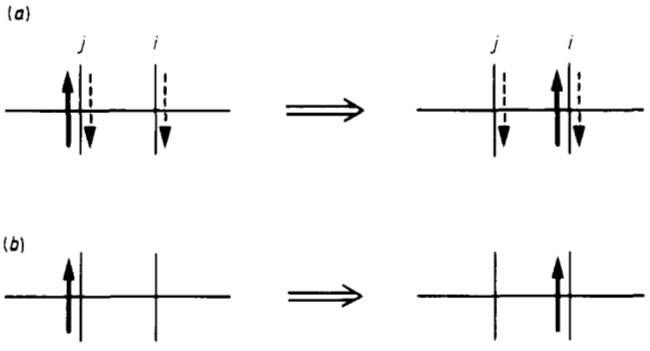

Figure 1. The possible hopping processes (*a*) in the non-projected pairing state (3) and (*b*) in the projected BCS state (2). The spins with broken arrows are optional in the (*a*) configurations.

while that in the state $|\varphi_0\rangle$ is

$$[n_{j\uparrow}(1-n_{i\uparrow})n_{i\uparrow}(1-n_{j\uparrow})]^{1/2}.$$

$n_{i\sigma}$ are the average electron occupation numbers, ($n_i = \Sigma_\sigma n_{i\sigma}$) which are the same in the states $|\varphi\rangle$ and $|\varphi_0\rangle$, because of the spin symmetry of the wavefunctions. This leads to the result [21]

$$g_t = 2\delta/(1+\delta). \tag{4a}$$

To determine g_s, we consider the spin exchange process shown in figure 2. The spin–spin interaction occurs only when both sites are singly occupied. The probability for such a process in the state $|\varphi\rangle$ is $(n_{j\uparrow}n_{i\downarrow}n_{j\downarrow}n_{i\uparrow})^{1/2}$, while in the state $|\varphi_0\rangle$ it is

$$[n_{j\uparrow}(1-n_{j\downarrow})n_{i\downarrow}(1-n_{i\uparrow})n_{j\downarrow}(1-n_{j\uparrow})n_{i\uparrow}(1-n_{i\downarrow})]^{1/2}.$$

The same result is obtained for the z component interaction $S_i^z S_j^z$. Thus one finds†

$$g_s = 4/(1+\delta)^2. \tag{4b}$$

It is important to realise that the projection operator greatly enhances the spin–spin correlations. To further illustrate this point, we list in table 1 all the possible two-site states together with their weights and the contributions to the spin–spin correlation in the half-filled case.

Having determined the renormalisation factors, we can define a renormalised Hamiltonian given by

$$H' = g_t H_t + g_s H_s. \tag{5}$$

The energy of the system in the state $|\varphi\rangle$ can be evaluated as the expectation value of H' in the state $|\varphi_0\rangle$

$$W = \langle H'\rangle_0. \tag{6}$$

Equations (4)–(6) form the basis of our renormalised Hamiltonian approach, which is analogous to the approach used by Rice and Ueda [6] for the periodic Anderson model with the difference that here we make a further mean-field approximation. This is because in the context of the periodic Anderson Hamiltonian the most important physical effect is the renormalisation of the f-level to the Fermi surface and not the spin interaction, which would make an exact treatment of the effective Hamiltonian impossible.

To justify this approach, we have carried out Monte Carlo calculations. Figures 3–5 show the comparisons between the renormalised mean-field theory and the essentially exact MC results for these wavefunctions. The

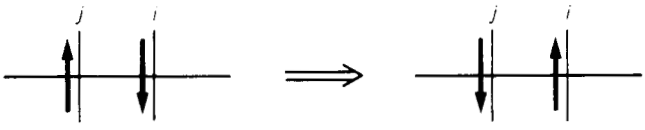

Figure 2. The spin exchange process in the states (2) and (3).

† In a systematic series expansion on δ and J/t, the higher-order terms of δ in (4) should be dropped away to be consistent with the effective Hamiltonian (1), where the higher-order terms are not included. This, however, does not change the qualitative physics discussed in this paper.

Table 1. This table illustrates the enhancement of the spin–spin correlation in the projected BSC state φ, equation (2), over that in the BCS state φ_0, (3), at half-filling. The weight of the configurations actually contributing to $\boldsymbol{S}_i \cdot \boldsymbol{S}_j$ increases by a factor of four due to the projection. The configurations at each site are denoted by 0 (empty state), ↑↓ (doubly occupied state), and σ (singly occupied state with spin σ).

Two-site configurations		No of configurations	Weight		Contribution to $S_i^+S_j^-$ or $S_i^-S_j^+$?
i	j		φ_0	φ	
0	0	1	$\frac{1}{16}$	0	—
σ	0	4	$\frac{1}{4}$	0	—
σ	σ	2	$\frac{1}{8}$	$\frac{1}{2}$	—
σ	$-\sigma$	2	$\frac{1}{8}$	$\frac{1}{2}$	yes
↑↓	0	2	$\frac{1}{8}$	0	—
↑↓	σ	4	$\frac{1}{4}$	0	—
↑↓	↑↓	1	$\frac{1}{16}$	0	—

quantitative agreement is within 5–15%, while the qualitative agreement is excellent for the wavefunction (2).

After replacing the projection operator, the energy of the system can be evaluated analytically. The variational task is to minimise W in (6). This leads to coupled gap equations, which we will derive and solve in the following sections.

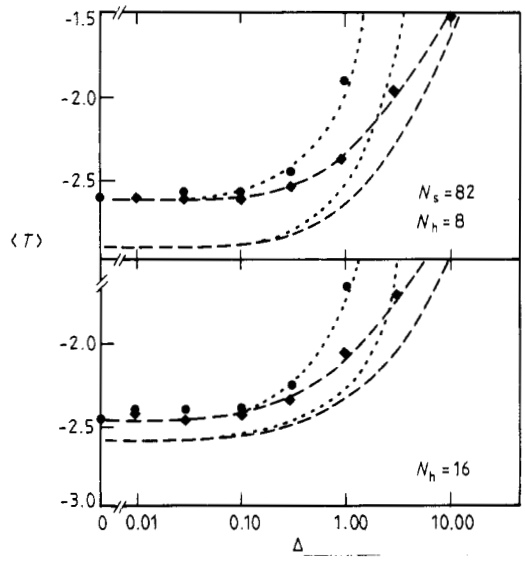

Figure 3. A comparison between the renormalised mean-field theory (RMF) (see (4)–(6)) and the Monte Carlo (MC) result for the kinetic energy $\langle T\rangle$ per hole in the projected BCS state (2). Both were calculated with a total number of sites $N_s = 82$ and a number of holes $N_h = 8$, 16. The variational parameter Δ is related to the parameters of the state (2) by

$$\frac{v_k}{u_k} = \frac{\Delta_k}{\varepsilon_k - \mu_0 + [\Delta_k^2 + (\varepsilon_k - \mu_0)^2]^{1/2}}$$

where μ_0 is a parameter, and ε_k is given by (8*b*). In the d-wave pairing state, $\Delta_k = \Delta(\cos k_x - \cos k_y)$ and in the s-wave state, $\Delta_k \equiv \Delta$. The full circles and squares are the MC results for the s- and d-waves respectively. The dotted and broken curves through the MC results are guides for the eyes. The second pair of dotted and broken curves are the results from RMF for s- and d-waves respectively.

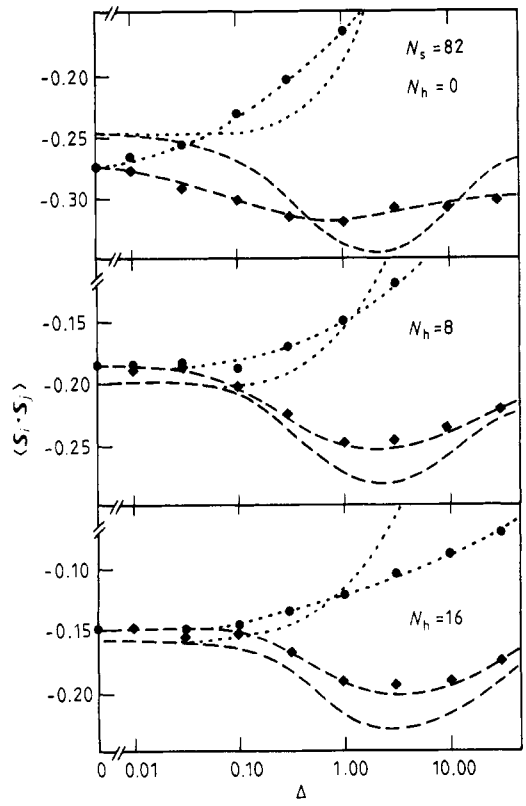

Figure 4. A comparison between the renormalised mean-field theory ((4)–(6)) (RMF) and Monte Carlo (MC) results for the nearest neighbour spin–spin correlation $\langle \boldsymbol{S}_i \cdot \boldsymbol{S}_j \rangle$ in the projected BCS state (2). Both were calculated with a total number of sites $N_s = 82$ and a number of holes $N_h = 0, 8, 16$. The variational parameter Δ is related to the parameters at the state (2) by

$$\frac{v_k}{u_k} = \frac{\Delta_k}{\varepsilon_k - \mu_0 + [\Delta_k^2 + (\varepsilon_k - \mu_0)^2]^{1/2}} .$$

where μ_0 is a parameter and ε_k is given by (8*b*). In the d-wave pairing state, $\Delta_k = \Delta(\cos k_x - \cos k_y)$ and in the s-wave state $\Delta_k = \Delta$. The full circles and squares are the MC results for the s- and d-waves respectively. The dotted and broken curves through them are guides for the eyes. The second pair of dotted and broken curves are the results from RMF for the s- and d-waves respectively.

3. Gap equations

In this section we derive the gap equations for the projected BCS wavefunction within the renormalised Hamiltonian scheme described in §2. We consider only the even-parity case, i.e., $u_{-k} v^*_{-k} = u_k v^*_k$, and $|v_{-k}|^2 = |v_k|^2$.

Evaluating (6), we obtain

$$W = 2g_t \sum_k \varepsilon_k |v_k|^2 + N_s^{-1} \times \sum_{k,k'} V_{k-k'} (|v_k|^2 |v_{k'}|^2 + u_k v^*_k v_{k'} u^*_{k'}) \tag{7}$$

where N_s is the total number of sites, and

$$V_k = -\tfrac{3}{4} g_s J \gamma_k \tag{8a}$$

$$\varepsilon_k = -t\gamma_k \tag{8b}$$

$$\gamma_k = 2(\cos(k_x) + \cos(k_y)) \tag{8c}$$

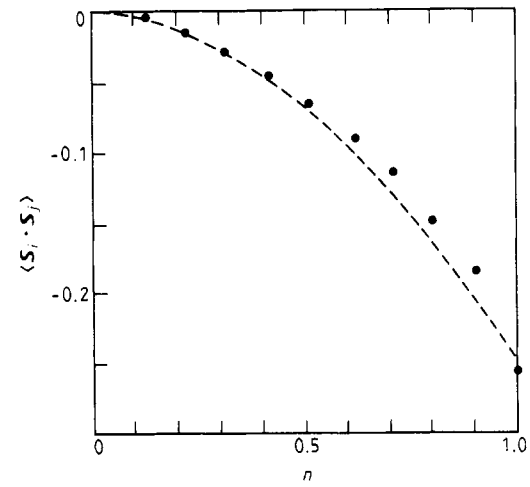

Figure 5. The nearest neighbour spin–spin correlation function $\langle \boldsymbol{S}_i \cdot \boldsymbol{S}_j \rangle$ as a function of electron filling in the projected Fermi liquid state ($u_k v_k = 0$ in (2)). The renormalised mean-field theory ((4)–(6)) (RMF), broken curve, agrees well with the Monte Carlo (MC), full circles, result in the entire filling region.

Note that ε_k and V_k have the same functional form, since H_s is derived by kinetic exchange. The electron number operator $N = \Sigma_{k\sigma} c^+_{k\sigma} c_{k\sigma}$ has expectation value $\langle N \rangle = 2\Sigma_k |v_k|^2$.

Let μ be the chemical potential of the system, the quantity we want to minimise is

$$\tilde{W} = \langle H' - \mu N \rangle_0 .$$

While minimising $\tilde{W}$ with respect to u_k and v_k for fixed μ, one must remember that H' is also a function of δ due to the renormalisation factors, and hence a function also of v_k. Carrying out this procedure, we find that

$$|u_k|^2 = \tfrac{1}{2}(1 + \xi_k/E_k) \tag{9a}$$

$$|v_k|^2 = \tfrac{1}{2}(1 - \xi_k/E_k) \tag{9b}$$

and

$$u_k v^*_k = \tilde{\Delta}_k / 2E_k \tag{9c}$$

where

$$E_k = (\xi_k^2 + |\tilde{\Delta}_k|^2)^{1/2} . \tag{9d}$$

The parameters $\tilde{\Delta}_k$ and ξ_k are dimensionless, and they are related to the particle–particle and particle–hole pairing amplitudes respectively

$$\tilde{\Delta}_k = \tilde{\Delta}_x \cos(k_x) + \tilde{\Delta}_y \cos(k_y)$$

$$\tilde{\xi}_k = \bar{\varepsilon}_k - \xi_x \cos(k_x) - \xi_y \cos(k_y) \tag{10}$$

where

$$\bar{\varepsilon}_k = (g_t \varepsilon_k - \tilde{\mu})/(\tfrac{3}{4} g_s J)$$

and $\tilde{\mu}$ is related to the chemical potential μ by

$$\mu = \tilde{\mu} - N_s^{-1} \left\langle \frac{\partial H'}{\partial \delta} \right\rangle_0 . \tag{11}$$

In (10)

$$\tilde{\Delta}_\tau = \langle c_{i\uparrow}^\dagger c_{i+\tau\downarrow}^\dagger - c_{i\downarrow}^\dagger c_{i+\tau\uparrow}^\dagger \rangle_0 \tag{12}$$

$$\xi_\tau = \sum_\sigma \langle c_{i\sigma}^\dagger c_{i+\tau,\sigma} \rangle_0 \tag{13}$$

with $\tau = x$ and y, $i + \tau$ denotes the NN of i in the τ direction. Since we consider the even-parity case, ξ_τ is real, but $\tilde{\Delta}_\tau$ can be complex. $\tilde{\Delta}_k$ and ξ_k satisfy the following coupled gap equations:

$$\tilde{\Delta}_k = N_s^{-1} \sum_{k'} \gamma_{k-k'} \tilde{\Delta}_{k'}/(2E_{k'})$$

$$\xi_k = \bar{\varepsilon}_k + N_s^{-1} \sum_{k'} \gamma_{k-k'} \xi_{k'}/(2E_{k'}). \tag{14}$$

The first one is the same as the usual BCS gap equation. The second one originates from the particle–hole correlation. From (12), it is clear that $\tilde{\Delta}_k$ is related to the pairing in the unprojected state $|\varphi_0\rangle$. It describes the 'smearing' of the pseudo-Fermi surface. However, $\tilde{\Delta}_k$ is not the superconducting order parameter in the projected state $|\varphi\rangle$ in our theory. E_k turns out to be the quasi-particle excitation energy (in units of $\frac{3}{4}g_s J$) in the pairing state as we will show in §5.

The coupled gap equations (14) are the basic equations in our approach. They can also be written in the x and y component form:

$$\tilde{\Delta}_\tau = N_s^{-1} \sum_k \cos(k_\tau)\tilde{\Delta}_k/E_k$$

$$\xi_\tau = -N_s^{-1} \sum_k \cos(k_\tau)\xi_k/E_k. \tag{15}$$

The gap equations must be solved simultaneously with the hole concentration equation, $\delta = N_s^{-1} \Sigma_k \xi_k/E_k$.

Before we discuss the non-trivial solutions, we note that $\tilde{\Delta}_k = 0$ is a trivial solution of the gap equations. This corresponds to the projected Fermi-liquid state. In this case, ξ_k changes sign at the Fermi surface. The parameters $\xi_x = \xi_y$ $(= \xi)$ are given by

$$\xi = N_s^{-1} \sum_{\xi_k \leq 0} \cos(k_x) + \cos(k_y).$$

The volume of the Fermi sea is determined by the number of electrons. The energy per site is

$$w = -4g_t t\xi - \tfrac{3}{4}g_s J\xi^2.$$

In particular, $w = -48/\pi^4 J \simeq -0.49J$ in the half-filled case. It will be shown in the next section that this trivial solution is unstable against the pairing states with $\tilde{\Delta}_k \neq 0$.

4. Solutions of the gap equations—half-filled case

At the half-filling, $\delta = 0$, $\tilde{\mu} = 0$, and there is no kinetic energy. We are interested in the possible lowest energy states of the solution of (14). The total energy of the system has a simple form in this case by use of (7) and (14)

$$W = -\tfrac{3}{8}g_s J \sum_k E_k.$$

Therefore the lowest energy states correspond to the maximum value of $\Sigma_k E_k$. For this reason, we use an *ansatz* for E_k to examine the solutions of the gap equations†

$$E_k = C(\cos^2(k_x) + \cos^2(k_y))^{1/2} \tag{16}$$

where C is a parameter to be determined. Note that such a choice gives only four point zeros for E_k. The gap equations then reduce to a single equation, and we get

$$C = \frac{1}{2N_s} \sum_k (\cos^2(k_x) + \cos^2(k_y))^{1/2}$$

which has numerical value $C \simeq 0.479$. The energy per site is

$$w = -\tfrac{3}{4}g_s J C^2 = -0.688J.$$

This energy is much lower (about 20%) than that of the projected Fermi-liquid state found above. The parameter $\tilde{\Delta}_k$ describes the pairing correlation in the renormalised Hamiltonian. Finite values of $\tilde{\Delta}_k$ indicate the binding of the electron pairs in the pairing states (3).

We now determine the parameters $\tilde{\Delta}_\tau$ and ξ_τ required for the choice of E_k in (16). Using (9*d*) and (10), we find that they should satisfy the following simultaneous equations:

$$\xi_x^2 + |\tilde{\Delta}_x|^2 = \xi_y^2 + |\tilde{\Delta}_y|^2 = C^2$$

$$2\xi_x \xi_y + (\tilde{\Delta}_x \tilde{\Delta}_y^* + \text{HC}) = 0. \tag{17}$$

There is a wide class of parameters which satisfy the conditions (17). All the states in this class give the same expectation value of the renormalised Hamiltonian H' in (5). Therefore at the half-filling, H' has a large degeneracy of ground states. For real $\tilde{\Delta}_x$ and $\tilde{\Delta}_y$, these states can be illustrated diagrammatically as shown in figure 6(*a*). A few examples of these states are

d-wave pairing:

$$\tilde{\Delta}_x = -\tilde{\Delta}_y = \xi_x = \xi_y = C/\sqrt{2} \tag{18a}$$

d-wave density matrix:

$$\tilde{\Delta}_x = \tilde{\Delta}_y = \xi_x = -\xi_y = C/\sqrt{2} \tag{18b}$$

chiral state:

$$\tilde{\Delta}_x = -\mathrm{i}\tilde{\Delta}_y = C \qquad \xi_x = \xi_y = 0 \tag{18c}$$

anisotropic state:

$$\tilde{\Delta}_x = \xi_y = C \qquad \tilde{\Delta}_y = \xi_x = 0. \tag{18d}$$

We remark that the d-wave density matrix state is different from the extended s-wave state proposed by Baskaran, Zou and Anderson [8]. In their theory, the particle–hole amplitude $\langle c^+ c \rangle_0$ is not included, i.e. $\xi_x = \xi_y = 0$. Therefore their state has the same energy as the projected Fermi-liquid state. The d-wave pairing state was studied numerically in [17] and [18], and the chiral state was discussed in [10]. They belong to the solutions of the same gap equations in the present approach.

† There might be other solutions for the gap equations. We believe that the form of the energy given by (16) gives the lowest energy.

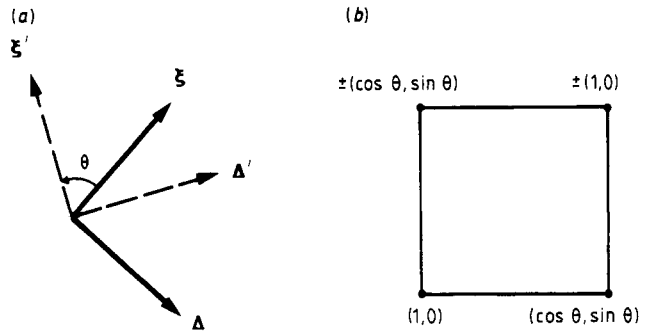

Figure 6. (*a*) Diagrammatic illustration of the degenerate ground states for the renormalised Hamiltonian (5) at half-filling. $\xi = \xi_x\hat{x} + \xi_y\hat{y}$, $\Delta = \tilde{\Delta}_x\hat{x} + \tilde{\Delta}_y\hat{y}$, with ξ_τ, $\tilde{\Delta}_\tau$ given by (12) and (13). The full arrows represent the d-wave pairing state with $\xi \perp \Delta$, and $|\xi| = |\Delta|$. All the states in (17) with the real parameters $\tilde{\Delta}_\tau$ may be obtained by rotating ξ and Δ simultaneously by angles θ, or reflecting the two vectors about the $\hat{x}$ axis. (*b*) An illustration of the SU(2) gauge transformation. A state described by (ξ', Δ') in (*a*) can be obtained by a local SU(2) from the state (ξ, Δ), under which $c_{i\sigma}^{\dagger}$ at the four sites of the plaquette transform according to (19), with (α_i, β_i) as denoted. The minus sign in front of the parentheses corresponds to the states in (*a*) after a reflection about the *x* axis. The transformation operator $c_{i\sigma}$ at other lattice sites is determined by a translation.

The degeneracy of the ground states of H' may be explained using the local SU(2) symmetry of the Heisenberg Hamiltonian H_s. This symmetry has been pointed out by Anderson [2]. Very recently Affleck and co-workers [22] have studied the invariance under a time-dependent SU(2) gauge transformation, and discussed the equivalence of some different mean-field theories. Here we wish to show that the symmetry described in (17) is a sub-group of the local SU(2), which preserves translational invariance and even parity that we imposed in deriving the gap equations.

Consider a local SU(2) gauge transformation, under which electron operators at site i transform as

$$\begin{aligned} c_{i\uparrow}^{\dagger} &\to \alpha_i c_{i\uparrow}^{\dagger} + \beta_i c_{i\downarrow} \\ c_{i\downarrow} &\to -\beta_i^* c_{i\uparrow}^{\dagger} + \alpha_i^* c_{i\downarrow} \end{aligned} \tag{19}$$

where $\alpha_i\alpha_i^* + \beta_i\beta_i^* = 1$. These are the particle–hole transformations with spin conservation. H_s, hence H' at half-filling is invariant under these transformations. Therefore all the states related by (19) are degenerate. A set of the parameters $\tilde{\Delta}_\tau$ and ξ_τ in our gap equations transforms to another set of the parameters under (19). The transformations corresponding to the degenerate state (17) derived from the gap equations are represented in figure 6(*b*), for real values of $\tilde{\Delta}_\tau$. There is also one to one correspondence to transformations of the d-wave pairing state to a state with complex $\tilde{\Delta}_\tau$ such as the chiral state (18*c*) with α and β complex.

Local U(1) gauge symmetry is a sub-group of the local SU(2) symmetry since it is of the form

$$c_{i\sigma} \to \tilde{c}_{i\sigma} = c_{i\sigma}\exp(\mathrm{i}\theta_i).$$

A general choice of θ_i transforms the BCS pairing state (3) to a non-BCS-type state, which has the same energy as the former. Since under such a transformation the Bloch coherence is lost, i.e. a state of the form

$$\tilde{c}_{k,\sigma} = \sum_j \exp(\mathrm{i}\boldsymbol{k}\cdot\boldsymbol{R}_j)\tilde{c}_{j,\sigma} = \sum_j \exp(\mathrm{i}\boldsymbol{k}\cdot\boldsymbol{R}_j + \mathrm{i}\theta_j)c_{j,\sigma}$$

is no longer a coherent superposition of the original states. Yet we can equally well pair $\tilde{c}_{k\uparrow}$ with $\tilde{c}_{-k\downarrow}^{+}$, and the energy would be the same as if we pair $c_{k\uparrow}^{+}$ with $c_{-k\downarrow}^{+}$. Thus the apparent coherent k-space pairing in the BCS wavefunction (3) is illusory. The absence of a coherent pairing order parameter at half-filling as a consequence of the U(1) gauge invariance has been stressed by Baskaran and Anderson [12].

It is important to realise that the states that are degenerate due to the SU(2) gauge symmetry are the unprojected states $|\varphi_0\rangle$ of (3), rather than the physical states $|\varphi\rangle$ which obey the strict local constraint. How does a projected state change under SU(2)? According to (19), a vacuum state (empty state) at site i must transform under SU(2) as

$$|0\rangle_i \to \mathrm{e}^{\mathrm{i}\theta_i}(\alpha_i^* - \beta_i^* c_{i\uparrow}^{\dagger} c_{i\downarrow}^{\dagger})|0\rangle_i.$$

This ensures that the vanishing of the state $c_{i\sigma}|0\rangle_i$ remains unchanged under the transformation as required physically. However a singly occupied electron state transforms under SU(2) as

$$c_{i\sigma}^{\dagger}|0\rangle_i \to \mathrm{e}^{\mathrm{i}\theta_i}c_{i\sigma}^{\dagger}|0\rangle_i.$$

At half-filling, each site is singly occupied. Therefore any half-filled state $|\varphi\rangle$ transforms into itself except for an overall phase factor under the SU(2) operator $\hat{U}$:

$$|\varphi\rangle \to \hat{U}|\varphi\rangle = \mathrm{e}^{\mathrm{i}\theta}|\varphi\rangle \qquad \theta = \sum_i \theta_i.$$

Although $\hat{U}$ does not commute with the projection operator P_d, we observe for the half-filled state $|\varphi_0\rangle$

$$\hat{U}P_d|\varphi_0\rangle = P_d\hat{U}|\varphi_0\rangle.$$

One way to see this is to notice that there is no empty site state also in $P_d|\phi_0\rangle$. Thus we can rewrite

$$P_d|\varphi_0\rangle = \prod_i (n_{i\uparrow} - n_{i\downarrow})^2|\varphi_0\rangle.$$

The SU(2) transformations all commute with the operator $(n_{i\uparrow} - n_{i\downarrow})^2$. Let $|\varphi\rangle = P_d|\phi_0\rangle$, and $|\varphi_0'\rangle = \hat{U}|\varphi_0\rangle$, then

$$P_d|\varphi_0'\rangle = P_d\hat{U}|\phi_0\rangle = \hat{U}|\varphi\rangle = \mathrm{e}^{\mathrm{i}\theta}|\phi\rangle = \mathrm{e}^{\mathrm{i}\theta}P_d|\varphi_0\rangle.$$

This proves explicitly that the two states $|\varphi_0\rangle$ and $|\varphi_0'\rangle$ related by any local SU(2) gauge transformation correspond to the same state $|\varphi\rangle$ except for a phase factor. *Therefore all the states in* (17) *correspond to the same physical state. The RVB ground state is non-degradable.*

There are also redundancies in the higher energy states in the fermion representation. For instance, the state of Baskaran, Zou and Anderson [8] at half-filled is identical to the projected Fermi liquid state, because the former transforms to the latter under (19) with $\alpha = 1$, $\beta = 0$ in one sublattice, and $\alpha = 0$, $\beta = 1$ in the other. This equivalence was also pointed out by Yokoyama and Shiba [18] in a different way.

We now comment on the local gauge symmetry in the original Hubbard model, which in terms of the original fermion operator is

$$H_{\mathrm{H}} = -t \sum_{\langle ij\rangle,\,\sigma} (d^{\dagger}_{i\sigma} d_{j\sigma} + \mathrm{HC}) + U \sum_{i} d^{\dagger}_{i\uparrow} d_{i\uparrow} d^{\dagger}_{i\downarrow} d_{i\downarrow}.$$

This Hamiltonian is not invariant under local gauge transformations with respect to the operators $d_{i\sigma}$. However, up to any finite order in t/U there exists a canonical transformation, which eliminates the doubly occupied sites [13]

$$H_{\mathrm{H}} \rightarrow H_{\mathrm{eff}} = \mathrm{e}^{\mathrm{i}S} H_{\mathrm{H}}\, \mathrm{e}^{-\mathrm{i}S}.$$

At half-filling, all the odd order terms in t/U vanish. The Hamiltonian is locally gauge invariant with respect to the electron operators in the new representation, i.e. the $c_{i\sigma}$ of (1) are Wannier operators of the old representation, $d_{i\sigma}$. Therefore the local gauge symmetry holds to any finite order in perturbation theory in t/U. This is the same as saying that the system has undergone a transition to a Mott insulator [13].

We have so far only examined the projected BCS-type trial wavefunctions. It is likely that the true ground state of the model Hamiltonian (1) at half-filled is the AF state [19]. Recently, Yokoyama and Shiba [18, 19] have studied a projected Hartree–Fock-type AF state. Using VMC they found the energy per site at half-filled to be $-0.642J$, slightly lower than $-0.636J$, the value found by Gros [17] in the d-wave pairing state by using a similar technique. However we may argue that the holes favour the pairing state away from half-filled because of the gain in kinetic energy. We have also applied the renormalised Hamiltonian approach to the AF states. Within this approximation, we find that at the half-filled, the AF state has higher energy than the RVB state (2), in contrast with the VMC results. We present the derivation and the results in Appendix 1.

5. Non-half-filled case

5.1. Ground state

Firstly we examine the energy needed to create propagating Bloch states. The simplest states for holes have the form

$$|\Phi_{i\sigma}\rangle = c_{i\sigma}|\varphi\rangle$$

which destroys a real electron at site i. We may also make a propagating Bloch state for the hole of the form

$$|\Phi_{p\sigma}\rangle = c_{p\sigma}|\varphi\rangle. \tag{20}$$

A rigorous calculation is possible at half-filling.

We consider any translationally invariant spin singlet state $|\varphi\rangle$ at half-filling. Let us denote by α the NN spin–spin correlation in $|\varphi\rangle$, $\alpha = \langle \boldsymbol{S}_l \cdot \boldsymbol{S}_j\rangle_{\varphi}$. Then the magnetic energy loss of a hole in the state $\Phi_{i\sigma}$ is $-4\alpha J$, because the four bonds connecting the site i are mixing. Since the matrix of H_{s} in (2) between any states $|\Phi_{i\sigma}\rangle$ and $|\Phi_{j\sigma}\rangle$ is diagonal, the moving hole state of (20) has the same magnetic energy as in $|\Phi_{i\sigma}\rangle$.

The kinetic energy of the hole in (20) is given by

$$\langle H_{\mathrm{t}}\rangle_{p} = 2t \sum_{\langle ij\rangle} \langle n_{i\sigma} n_{j\sigma} + S^{+}_{i} S^{-}_{j}\rangle_{\varphi} \exp(\mathrm{i}\boldsymbol{p}\cdot\boldsymbol{R}_{ji}) + \mathrm{HC}$$

where $\langle\ \rangle_{\varphi}$ denotes the expectation value in the half-filled state. Using the fact that $\langle n_i n_j\rangle_{\varphi} = 1$, we get

$$\langle H_{\mathrm{t}}\rangle_{p} = t(1 + 4\alpha)(\cos(p_x) + \cos(p_y)). \tag{21}$$

Since $\alpha \simeq -0.33$ for the ground state, (21) gives a band width for a Bloch hole of $0.64|t|$. The minimum energy to remove an electron and create such a Bloch hole is $-0.32\,t - 4\alpha J$.

The Bloch states are not the lowest energy states of the holes however. We now apply the gap equations to study a system with a few pair of holes. The energy to create a pair of holes is -2μ by the definition of the chemical potential. Since the parameter $\tilde{\mu} = 0$ at the half-filled, (11) gives the energy per hole to be $N_{\mathrm{s}}^{-1}\langle \partial H'/\partial\delta\rangle_0$, a quantity related to the unprojected state $|\varphi_0\rangle$ at half-filling. In the presence of holes, the kinetic part of the Hamiltonian explicitly breaks the SU(2) and U(1) gauge symmetries, while the Heisenberg spin part remains invariant under these symmetries.

Using (4) and (5), for the states $|\varphi_0\rangle$ described by (17), the magnetic energy per hole is

$$\frac{1}{N_{\mathrm{s}}}\left(\frac{\partial g_{\mathrm{s}}}{\partial\delta}\right)\langle H_{\mathrm{s}}\rangle_0 = 6C^2 J$$

a value equivalent to the loss of four bonds in the spin–spin correlations, and it is the same for all these states as a consequence of the SU(2) gauge invariance of the spin part of the Hamiltonian H_{s}. The kinetic energy per hole in this case is given by

$$T = \frac{1}{N_{\mathrm{s}}}\left(\frac{\partial g_{\mathrm{t}}}{\partial\delta}\right)\langle H_{\mathrm{t}}\rangle_0 = -4t(\xi_x + \xi_y).$$

ξ_{τ} is the particle–hole correlation in $|\varphi_0\rangle$ as defined in (13). When the holes are introduced, a fraction (g_{t}) of this correlation becomes coherent in the state $|\varphi\rangle$. Therefore the larger values of ξ_{τ} correspond to the lower kinetic energy of the holes. But ξ_{τ} are subject to (17). The kinetic energy can be written in the following form by using (17):

$$T = -4t(2C^2 - |\tilde{\Delta}_x + \tilde{\Delta}_y|^2)^{1/2}\ \mathrm{sgn}(\xi_x + \xi_y).$$

Different parameters $\tilde{\Delta}_{\tau}$ and ξ_{τ} describe different states with different energies upon doping. The above hole kinetic energy expression immediately leads to the important conclusion that the d-wave pairing state, where $\tilde{\Delta}_x + \tilde{\Delta}_y = 0$ gives the best kinetic energy, which is

$$T_{\mathrm{d\ wave}} = -4(\sqrt{2})Ct = -2.71t.$$

Both the d-wave density matrix state (18*b*) and the chiral state (18*c*) have zero kinetic energies, and are not favoured upon doping. The kinetic energy for the d-wave pairing state in our analytical approach is quite close to the VMC result, where it is found to be $-2.55\ t$ for systems with 10% holes [17]. It is also substantially below the value found for a Bloch hole.

The introduction of some holes breaks the local gauge symmetry and causes the ground state to be coherent. The stable lowest energy state upon doping is the d-wave pairing state.

It is worthwhile remarking that in a Hubbard model it is the expectation value of the kinetic energy which determines the integrated optical weight associated with the charge carriers in the f-sum rule [23] and in the present case this optical weight is proportional to the number of holes with an optical mass determined from the proportionality constant of order at^{-1} (where a is the lattice constant).

The gap equations for the finite hole concentrations can be solved numerically. Here we shall consider only the most stable state—the d-wave pairing state. In this case, we set $\tilde{\Delta}_x = -\tilde{\Delta}_y = \tilde{\Delta}$, and $\xi_x = \xi_y = \xi$. The four equations (13) reduce to two because of the symmetry between the x and y components. These two equations uniquely determine $\tilde{\Delta}$ and ξ for the fixed values of t, J and $\tilde{\mu}$. The numerical results of the gap equations are plotted in figure 7 for $\tilde{\Delta}$ as a function of the hole concentration.

We now discuss the superconducting order parameter. As mentioned in §3, $\tilde{\Delta}$ is not the order parameter. The superconducting order parameter is

$$\Delta_{SC}(\boldsymbol{R}_{ij}) = \langle c_{i\uparrow}^{\dagger} c_{j\downarrow}^{\dagger} - c_{i\downarrow}^{\dagger} c_{j\uparrow}^{\dagger} \rangle$$

an expectation value in the projected state (2). This quantity describes the Cooper pairing in a real space representation. We shall adopt the Gutzwiller method to calculate this quantity. In analogy to the derivation for the hopping energy in §2 we find that the nearest-neighbour sites i and j

$$\langle c_{i\uparrow}^{\dagger} c_{j\downarrow}^{\dagger} \rangle = g_t \langle c_{i\uparrow}^{\dagger} c_{j\downarrow}^{\dagger} \rangle_0 .$$

Therefore for nearest-neighbour sites, the order parameter is related to the variational parameter $\tilde{\Delta}$ in the gap equations by

$$\Delta_{SC} = g_t \tilde{\Delta}. \tag{22}$$

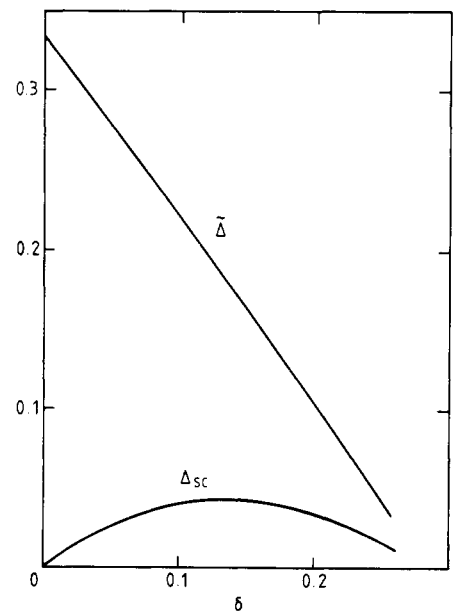

Figure 7. Variational parameter $\tilde{\Delta}$ and superconducting order parameter Δ_{SC} as functions of the hole concentration δ for a choice of $t/J = 5$ in the d-wave pairing state.

The value of Δ_{SC} as a function of δ is plotted in figure 7 in comparison with $\tilde{\Delta}$. Δ_{SC} vanishes linearly near $\delta = 0$. Δ_{SC} found in our theory is in good agreement with the Monte Carlo results [17]. The absence of the superconducting order parameter at half-filled obtained from (22) agrees with the discussion in §4 from the viewpoint of the local gauge symmetry.

The kinetic energy of holes in the AF state is found to be quite high in our analytic approach (see Appendix 1). However, the Gutzwiller approximation we adopted is too rough to determine whether a RVB or AF state has lower energy. Numerical results of VMC [17–19] suggest both the spin–spin correlation energy and the kinetic energy of the holes between the d-wave pairing state and the AF states are very close. The question which state is more favourable in energy remains unresolved.

5.2. Excited states and finite temperatures

We begin by examining the spin degrees of freedom in half-filled and near half-filled cases. An excited state can be created by applying the spin raising operator to a specific site to obtain

$$|\Psi_{i,+}\rangle = S_i^{\dagger} P_d |\varphi_0\rangle.$$

We can commute $S_i^{\dagger}$ with P_d to obtain

$$|\Psi_{i,+}\rangle = P_d S_i^{\dagger} |\varphi_0\rangle$$
$$= \sum_{\boldsymbol{p},\boldsymbol{p}'} \exp[i(\boldsymbol{p} - \boldsymbol{p}') \cdot \boldsymbol{R}_i] P_d \, c_{\boldsymbol{p}\uparrow}^{\dagger} c_{\boldsymbol{p}'\downarrow} |\varphi_0\rangle.$$

This state is therefore a superposition of two independent quasi-particle states similar to a metal where the low energy excitations are made up of superpositions of electron and hole states. The quasi-particle states (spinons) can be defined by

$$|\Psi_{\boldsymbol{p}\uparrow}\rangle = P_d c_{\boldsymbol{p}\uparrow}^{\dagger} \prod_{\boldsymbol{k}\neq\boldsymbol{p}} (u_{\boldsymbol{k}} + v_{\boldsymbol{k}} c_{\boldsymbol{k}\uparrow}^{\dagger} c_{-\boldsymbol{k}\downarrow}^{\dagger}) |0\rangle. \tag{23}$$

The quasi-particle energy $\bar{E}_{\boldsymbol{p}}$ is defined to be the difference of the expectation values of $K = H - \mu N$ in the state $|\psi_{\boldsymbol{p}\uparrow}\rangle$ and in the ground state $|\varphi\rangle$. We use the Gutzwiller method to calculate the energy of the state (23). The energy difference between the two states contains two parts. One is due to the changes of the renormalization factors g_t and g_s, the other comes from the change of the wavefunction itself. The former just cancels exactly the second term in μ in (11). Using (7) to calculate the energy difference due to the wavefunction change, we get

$$\bar{E}_{\boldsymbol{p}} = (1 - 2v_{\boldsymbol{p}}^2)\left(g_t \varepsilon_{\boldsymbol{p}} + N_s^{-1} \sum_{\boldsymbol{k}} V_{\boldsymbol{k}-\boldsymbol{p}} v_{\boldsymbol{k}}^2 - \tilde{\mu} \right)$$
$$+ 2u_{\boldsymbol{k}} v_{\boldsymbol{k}} N_s^{-1} \sum_{\boldsymbol{k}} V_{\boldsymbol{k}-\boldsymbol{p}} u_{\boldsymbol{k}}^{*} v_{\boldsymbol{k}}.$$

Applying the gap equations to simplify the expression, we obtain

$$\bar{E}_{\boldsymbol{p}} = \tfrac{3}{4} g_s J E_{\boldsymbol{p}}. \tag{24}$$

Note this energy is independent of the local SU(2) gauge and does not depend on the particular fermion representation. At the pseudo-Fermi surface, where by definition $\xi_p = 0$, we have $E_p = |\tilde{\Delta}_p|$. Since the state (23) breaks a pair of electrons, $\bar{E}_p$ describes the binding energy of the pair at the pseudo-Fermi surface. The excitation energy depends on the particular RVB. For the Fermi liquid state ($u_k v_k = 0$) then $\bar{E}_p = 0$ over the whole pseudo-Fermi surface. However in the ground RVB state it vanishes only at four points, e.g. when $n = 1$, $\bar{E}_p = E_p = 0$, if $(p_x, p_y) = (\pm\pi/2, \pm\pi/2)$ and the density of spinon states at low energies is

$$N(\bar{E}) = \sum_p \delta(\bar{E} - \bar{E}_p) \rightarrow \frac{2\bar{E}}{\pi(\frac{3}{4}g_s J)^2} \qquad \text{as } \bar{E} \rightarrow 0.$$

We turn now to a brief discussion of the system at finite temperature. The extension of the mean-field gap equations to finite T is not so straightforward. The existence of a finite $\tilde{\Delta}_k$ is controlled by the energy scale of $\bar{E}_k$ i.e. by J in (24). On the other hand if we consider the limit $\delta \ll 1$ there is a very small energy scale $\propto \delta t$ which controls the definition of a coherent gauge. In other words it is only the kinetic energy which allows us to determine the gauge uniquely and at temperatures $J \gg T \gg \delta t$, the gauge coherence will be lost. Yet in this temperature range the magnetic coherence survives since as we have stressed earlier this is independent of the choice of gauge on each site. The properties of the system in this temperature region are clearly very different from Fermi liquid behaviour as Anderson has stressed and these two energy scales should correspond to his 'holon' and 'spinon' energy scales respectively. The thermopower should obey the Heikes formula [24] and we can expect only a low mobility of the holes. However, a more detailed study of this regime is required.

6. Discussion

We have used a variational method to study a projected BCS trial wavefunction for the square lattice effective Hamiltonian. Using a Gutzwiller approximation to treat the effect of the projection operator, we obtained a renormalised Hamiltonian in which the projection operator is replaced by renormalisation factors. This approximation is shown to be in good agreement with numerical Monte Carlo calculations for such projected wavefunctions. In this mean-field approximation both particle–particle and particle–hole pairing amplitudes must be included. The fermion representation for the ground state at the half-filled band is highly redundant, due to a local SU(2) invariance at exactly half-filling. This redundancy is reflected in an apparent degeneracy of the BCS trial wavefunction before projection. Doping destroys the local SU(2) invariance and splits these degenerate states, and we find that the stable state upon doping is the d-wave pairing RVB state. In this RVB state, electrons are paired even at half-filling and it costs an energy of order J to break a pair. These pre-existing electron pairs lead to a non-zero superconductivity amplitude upon doping, and the magnitude of this superconducting amplitude or order parameter is shown to be proportional to the hole concentration δ when δ is small. The elementary excitations at half-filling are the projected BCS quasi-particle states or spinons, with four point zeros on the pseudo-Fermi surface.

Our analytic approach can also be applied to 1D and systems with dimensionality $d \geqslant 3$. We find that lowest energy state in 1D is the projected Fermi liquid RVB without electron pairing, as shown in Appendix 2. Our theory predicts no superconductivity in a 1D RVB. For large d, the energy per bond in the RVB pairing state is proportional to $1/d$, reduces relative to an AF. So the pairing state is particularly favourable in 2D. The precise form of the 2D phase diagrams which depends sensitively on the relative energies of the AF and d-wave RVB states as a function of δ is too subtle a question to be settled by the approximation we use here.

There are many questions that require further investigation such as the exact relationship between the discussion here in terms of phase coherence among the paired electrons and Anderson's 'holon' [25] concept or the nature of the high-temperature phase where this phase coherence is lost but strong magnetic correlations remain and presumably do not lead to a Fermi liquid that is the usual description of a normal state.

Acknowledgments

We would like to thank D Poilblanc, R Joynt, M Roos, T K Lee, G Kotliar for many useful discussions. Financial support from the Swiss Nationalfonds is gratefully acknowledged.

Appendix 1: The projected spin-density-wave state

In this Appendix, we use the renormalised Hamiltonian approach to study the projected spin-density-wave state for effective Hamiltonian (1). That state was proposed and studied using VMC by Yokoyama and Shiba [18]. The generalisation of the Gutzwiller method to the antiferromagnetic states for the hopping process was formulated by Ogawa and co-workers [26].

The projected spin-density-wave state [18, 19] is

$$|\psi\rangle = P_d |\psi_0\rangle \qquad \text{(A1.1)}$$

$$|\psi_0\rangle = \prod_{k\sigma} (u_k c^\dagger_{k\sigma} + \sigma v_k c^\dagger_{k+Q,\sigma})|0\rangle \qquad \text{(A1.2)}$$

where k runs over the Fermi sea, $Q = \pi/a\,(1, 1)$, and

$$u_k = [(1 + \cos\theta_k)/2]^{1/2}$$

$$v_k = [(1 - \cos\theta_k)/2]^{1/2}$$

$$\cos\theta_k = \gamma_k/(\Delta^2_{AF} + \gamma^2_k)^{1/2}.$$

Δ_{AF} is a variational parameter, and γ_k is given by (8*c*).

In a study of the expectation value in the state (A1.1), we use the Gutzwiller approximation to replace the projection operator by renormalisation factors. In analogy to the analysis we discussed in §2, we find that

$$g_t = \frac{1-n}{1-2n_\uparrow n_\downarrow/n}$$

$$g_s = (1-2n_\uparrow n_\downarrow/n)^{-2}$$

where $n_\uparrow$ and $n_\downarrow$ are the spin-up and spin-down electron occupation number of state $|\psi_0\rangle$ in one sublattice respectively. The renormalisation factors reduce to (4) in the case $n_\uparrow = n_\downarrow$, and the form for g_t agrees with [26].

Within this scheme, we obtain the energy per site at half-filling

$$w = -2J(a^2 + 6b^2)/(1+a^2)^2$$

where

$$a = N_s^{-1} \sum_k \Delta_{AF}/(\Delta_{AF}^2 + \gamma_k^2)^{1/2}$$

$$b = (8N_s)^{-1} \sum_k \gamma_k^2/(\Delta_{AF}^2 + \gamma_k^2)^{1/2}.$$

The spin–spin correlation $\langle S_i \cdot S_j \rangle = \frac{1}{2}w$, and the staggered magnetisation is

$$M_s = \bar{n}_\uparrow - \bar{n}_\downarrow = 2a/(1+a^2)$$

with $\bar{n}_\sigma$ the occupation number in the state $|\psi\rangle$. $\langle S_i \cdot S_j \rangle$ and M_s are plotted in figure A1 as functions of Δ_{AF}. Figure A1 also shows the VMC calculations [18]. The case $\Delta_{AF} = 0$ corresponds to the projected Fermi liquid state, while $\Delta_{AF} \to \infty$ corresponds to the Néel state. The results agree well for large values of Δ_{AF}, but there are substantial deviations for small Δ_{AF}.

The kinetic energy per hole in our theory is

$$T = -16tb/(1+a^2).$$

For the optimal value of Δ_{AF} (~ 0.9), $T = -2.16t$, substantially higher than that in the d-wave pairing state. Note that this value is also higher than that found in the VMC calculation [18], where the optimal Δ_{AF} is found to be much smaller.

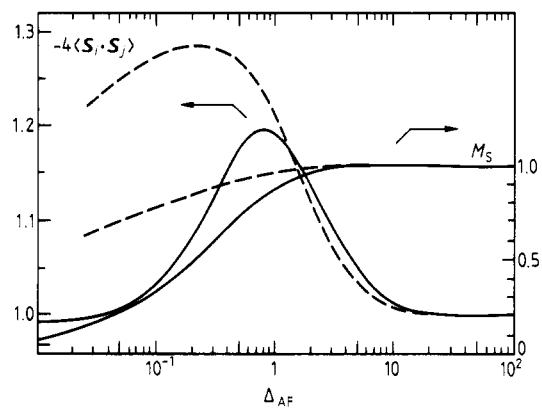

Figure A1. Spin–spin correlation and staggered magnetisation M_s as functions of Δ_{AF} in the projected spin-density-wave state. The full curves are the results of the renormalised Hamiltonian approach, and the broken curves are the VMC results (extrapolated to the infinite systems) by Yokoyama and Shiba [18, 19].

Appendix 2. RVB in a 1D system

The renormalised Hamiltonian approach can be straightforwardly applied to the model (1) in 1D. Using the projected BCS wavefunction (2), and the same technique for 2D, we have found that the RVB ground state at the half-filling is described by an equation between ξ_x and $\tilde{\Delta}_x$ (defined in (12)–(13)):

$$|\tilde{\Delta}_x|^2 + \xi_x^2 = C_1^2 \qquad \text{(A2.1)}$$

with

$$C_1 = (2N_s)^{-1} \sum_{k_x} |\cos(k_x)| = 2/\pi^2$$

(A2.1) is parallel to (17) in 2D. Similar to the 2D case, different parameters in (A2.1) are related to each other under the SU(2) gauge transformation, and correspond to the same physical state. This state is described by the projected Fermi liquid state, where $\tilde{\Delta}_x = 0$, $\xi_x = C_1$. Earlier Monte Carlo calculations [27] and more recent exact calculation [28] with this wavefunction have shown that the energy of this state is extremely close to the exact solution [29]. The energy per site in our analytic mean-field approach is $-6/\pi^2$. This value deviates by about 37% from the true result [27, 28]. This quantitative discrepancy however is not surprising, because the Gutzwiller approximation is poor in 1D.

In parallel to the discussion in §4, we can study the system with some holes. We found that the stable lowest-energy state corresponds to $\tilde{\Delta}_x = 0$. Introducing the finite value of $\tilde{\Delta}_x$, the system loses kinetic energy. Therefore we expect there is no electron pairing and no superconductivity in this 1D RVB.

References

[1] Anderson P W 1987 *Science* **235** 1196
[2] Anderson P W 1988 in *Proc. Int. Enrico Fermi School of Phys. (1987)* (Amsterdam: North Holland) at press
[3] Rice T M 1987 *Z. Phys.* B **67** 141
[4] Zhang F C and Rice T M 1988 *Phys. Rev.* B **37** 3759
[5] Gutzwiller M C 1963 *Phys. Rev. Lett.* **10** 159
[6] Rice T M and Ueda K 1985 *Phys. Rev. Lett.* **55** 997; 1986 *Phys. Rev.* B **34** 6420
[7] Kotliar G and Ruckenstein A E 1986 *Phys. Rev. Lett.* **57** 1362
[8] Baskaran G, Zou Z and Anderson P W 1987 *Solid State Commun.* **63** 973
[9] Ruckenstein A, Hirschfeld P and Appel J 1987 *Phys. Rev.* B **36** 857
Cyrot M 1987 *Solid State Commun.* **62** 821
Isawa Y, Maekawa S and Ebisawa H 1987 *Physica* B **148** 391
Müller-Hartmann E, Drzazga M, Kampf A and Wischman H A 1987 *Preprint*
[10] Kotliar G 1988 *Phys. Rev.* B **37** 3664
[11] Suzumura Y, Hasegawa Y and Fukuyama H 1988 *Preprint*
[12] Baskaran G and Anderson P W 1988 *Phys. Rev.* B at press

[13] Kohn W 1964 *Phys. Rev.* **133** A171
Brinkman W F and Rice T M 1970 *Phys. Rev.* B **2** 4302
Chao K A, Spalek J, and Oles A M 1977 *J. Phys. C: Solid State Phys.* **10** L271
Hirsch J E 1985 *Phys. Rev. Lett.* **54** 1317
MacDonald A H and Girvan S 1987 *Preprint*
[14] Vaknin D *et al* 1987 *Phys. Rev. Lett.* **58** 2802
Shirane G *et al* 1987 *Phys. Rev. Lett.* **59** 1613
[15] Horsch P and Kaplan T A 1983 *J. Phys. C: Solid State Phys.* **16** L1203
[16] Gros C, Joynt R and Rice T M 1987 *Z. Phys.* B **68** 425
[17] Gros C 1988 *Phys. Rev.* B at press
[18] Yokoyama H and Shiba H *J. Phys. Soc. Japan* **56** 3570
[19] Yokoyama H and Shiba H 1988 *Preprint*
[20] Oitmaa J and Betts D D 1978 *Can. J. Phys.* **56** 897
[21] Vollhardt D 1984 *Rev. Mod. Phys.* **56** 99
[22] Affleck I, Zou Z, Hsu T and Anderson P W 1988 *Preprint*
[23] Baeriswyl D, Gros C and Rice T M 1987 *Phys. Rev.* B **35** 1891
[24] Mott N 1974 in *Metal-Insulator Transitions* (London: Taylor and Francis)
[25] Kivelson S, Rokshar D and Sethna J 1987 *Phys. Rev.* B **35** 8865
[26] Ogawa T, Kanda K and Matsubara T 1975 *Prog. Theor. Phys.* **53** 614
[27] Gros C, Joynt R and Rice T M 1987 *Phys. Rev.* B **36** 381
[28] Gebhard F and Vollhardt D 1987 *Phys. Rev. Lett.* **59** 1472
[29] Bethe H 1931 *Z. Phys.* **71** 205